Up- and Down-Conversion

International Edition: DOI: 10.1002/anie.201604682
German Edition: DOI: 10.1002/ange.201604682

Constructing Interfacial Energy Transfer for Photon Up- and Down-Conversion from Lanthanides in a Core–Shell Nanostructure

Bo Zhou, Lili Tao, Yang Chai, Shu Ping Lau, Qinyuan Zhang,* and Yuen Hong Tsang**

Abstract: *We report a new mechanistic strategy for controlling and modifying the photon emission of lanthanides in a core–shell nanostructure by using interfacial energy transfer. By taking advantage of this mechanism with Gd^{3+} as the energy donor, we have realized efficient up- and down-converted emissions from a series of lanthanide emitters (Eu^{3+}, Tb^{3+}, Dy^{3+}, and Sm^{3+}) in these core–shell nanoparticles, which do not need a migratory host sublattice. Moreover, we have demonstrated that the Gd^{3+}-mediated interfacial energy transfer, in contrast to energy migration, is the leading process contributing to the photon emission of lanthanide dopants for the $NaGdF_4$@$NaGdF_4$ core–shell system. Our finding suggests a new direction for research into better control of energy transfer at the nanometer length scale, which would help to stimulate new concepts for designing and improving photon emission of the lanthanide-based luminescent materials.*

Controlling photon emission of lanthanide-doped nanomaterials has been a key research topic in recent years owing to their broad applications ranging from solid-state lasers, displays, photovoltaics, nanophotonics, to biological imaging and therapy.[1] The unique 4f electronic configuration of trivalent lanthanide ions enables them a great optical capability in photon manipulation, of which the infrared-to-visible up-conversion is a typically investigated process.[1a,2] The photon up-conversion also benefits much from the nano-sized crystalline lattice owing to its extremely low phonon energy, which can effectively minimize non-radiative decays, such as multi-phonon relaxation.[2b,3] So far, up-conversion emissions spanning from near-ultraviolet to near-infrared spectral regions have been readily accessible in lanthanide-doped nanocrystals by approaches including tuning the emitters and sensitizers (and their concentration ratio), tailoring crystal field, adopting unique nanostructure designs.[4] Moreover, intense ultraviolet-to-visible down-conversion has also been achieved in lanthanide-doped nanocrystals by employing suitable lanthanide dopants (e.g., Tb^{3+} and Eu^{3+}) and sensitizing system (e.g., Ce^{3+}), as evident in recent progress.[5] However, for these luminescent materials the lanthanide dopants are usually doped in a homogeneous way during the synthetic experiments, making their emission performance suffer from deleterious luminescence quenching because of the strong interactions between them (e.g., cross-relaxation).[2] On the other hand, limited by the intrinsic electronic configuration, traditionally efficient photon up-conversion can only be achieved in Er^{3+}, Tm^{3+}, and Ho^{3+} through a typical process of energy-transfer up-conversion by employing Yb^{3+} or Nd^{3+} as the sensitizer.[1a,2] While this process does not work well for the other lanthanide ions because of the lack of long-lived intermediate states to store the energy, and some other approaches, such as cooperative sensitization, still result in much weak emission.[2] Therefore, it is of great significance for exploring new mechanisms to realize efficient photon up- and down-conversion emission of more lanthanide ions as well as a new way for minimizing the concentration quenching of the lanthanide-based luminescent materials.

Herein, we propose a new mechanistic strategy to achieve photon up- and down-conversion through the use of Gd^{3+}-mediated interfacial energy transfer (IET) within a core–shell structure, as illustrated in Figure 1. In our design, Gd^{3+} is selected as the energy donor which can be activated by the ultraviolet and infrared irradiation through employing Ce^{3+} and Yb^{3+}/Tm^{3+} as sensitizers (Figure 1b and Figure S1 in the Supporting Information). The energy donor, sensitizer, and lanthanide emitter ions are separately incorporated into a core–shell architecture at different layers (Figure 1a). This not only allows us to manipulate the energy interactions in a precisely controlled way but also helps to minimize the non-radiative decays, such as cross-relaxation by a spatial separation of the dopants.[1e,4d,f] To effectively exclude any possibility of optical affection on photon emission (e.g., energy migration), optically inert hexagonal phase $NaYF_4$ is selected as the shell matrix, which is also shown to be a good host for lanthanides with efficient photon down-conversion besides up-conversion.[3,6] By taking advantage of the IET mechanism, multiple visible emissions from a series of lanthanide ions (Eu^{3+}, Tb^{3+}, Dy^{3+}, and Sm^{3+}) are possible at both up- and down-conversion pump schemes.

We first prepared the $NaYbF_4$:Tm/Gd@$NaYF_4$:A (A = Eu, Tb, Dy, and Sm) core–shell nanoparticles by using a two-step coprecipitation method (see the Supporting Information).[4n] In a typical experiment, the $NaYbF_4$:Tm/Gd(1/

[*] Dr. B. Zhou, Dr. L. Tao, Dr. Y. Chai, Prof. S. P. Lau, Dr. Y. H. Tsang
Department of Applied Physics
The Hong Kong Polytechnic University
Hung Hom, Kowloon, Hong Kong (China)
E-mail: eebzhou@gmail.com
Yuen.Tsang@polyu.edu.hk
Prof. Q. Y. Zhang
State Key Laboratory of Luminescent Materials and Devices, and
Institute of Optical Communication Materials
South China University of Technology
Guangzhou, 510640 (China)
E-mail: qyzhang@scut.edu.cn
Dr. L. Tao
School of Materials and Energy, Guangdong University of Technology
Guangzhou, 510006 (China)

Supporting information for this article can be found under: http://dx.doi.org/10.1002/anie.201604682.

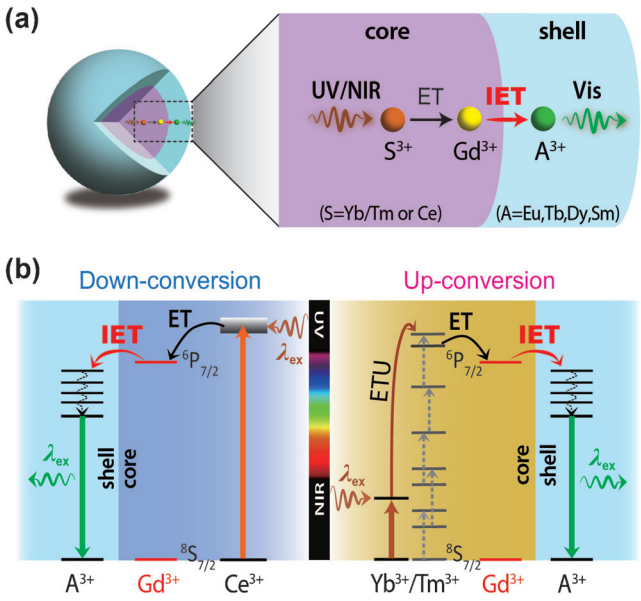

Figure 1. a) Proposed mechanism of photon up- and down-conversion through Gd^{3+}-mediated interfacial energy transfer in a core–shell architecture design. b) Schematic representation of energy-transfer processes involving a core–shell system with Yb^{3+}/Tm^{3+} and Ce^{3+} as sensitizers for harvesting near-infrared (NIR) and ultraviolet (UV) irradiation energy. ET = energy transfer, ETU = energy transfer up-conversion, and IET = interfacial energy transfer.

50 mol%) core nanoparticles were first synthesized as seeds, followed by an epitaxial growth of the $NaYF_4$:A (A = Eu, Tb, Dy, and Sm) shell layer. The as-synthesized core–shell nanoparticles have an average size of about 26.8 nm with a 4.0 nm thick shell layer (Figure 2a), and they are in hexagonal phase based on the X-ray diffraction profiles (Figure 2b) and Fourier transform diffraction pattern (Figure 2a; right bottom panel). These core–shell nanoparticles are in a single crystalline phase as evidenced by the clear lattice fringe exhibited in the high-resolution TEM image (Figure 2a; right top panel). Besides the increase in size, the core–shell structure was also confirmed by the EDS result that the elements in shell precursor were only observed for the samples after growing the shell layer (Figure 2c).

At 980 nm excitation, characteristic up-conversion emissions are clearly observed for these core–shell samples, as shown in Figure 2d and Figures S2,S3. For example, the typical emission bands of Eu^{3+} recorded at 591, 615, and 695 nm are from its optical transitions of $^5D_0 \rightarrow {}^7F_1$, $^5D_0 \rightarrow {}^7F_2$, and $^5D_0 \rightarrow {}^7F_4$, respectively. In contrast, no emission of lanthanide emitters from the shell layer was observed for the core–shell samples without Gd^{3+} being doped in the core (Figure S4). Also, the decay curves of Gd^{3+} emission measured at 311 nm ($^6P_{7/2} \rightarrow {}^8S_{7/2}$ transition) show a remarked decrease in lifetime for the core–shell samples comprising emitters in the shell layer (Figure S5). These results together confirmed that the lanthanide emitter in the shell layer is activated due to the interfacial energy transfer from the Gd^{3+} donor embedded in core (Figure S6).

Through the use of the Gd^{3+}-mediated IET mechanism, extensive, intense ultraviolet-to-visible down-conversion luminescence has also been realized for the $NaGdF_4$:Ce@$NaYF_4$:A (A = Eu, Tb, Dy, and Sm) core–shell samples at 254 nm excitation (Figure 2e and Figures S7–S9). Note that the down-conversion emission is markedly improved for the samples after removing the surface-capped oleic ligands which can trap the ultraviolet irradiation energy with resultant weak emissions (Figure S9).[5e] In the control experiment, we further investigated the emission properties of the samples with both lanthanide emitters and sensitizers homogenously codoped together in the core, for example,

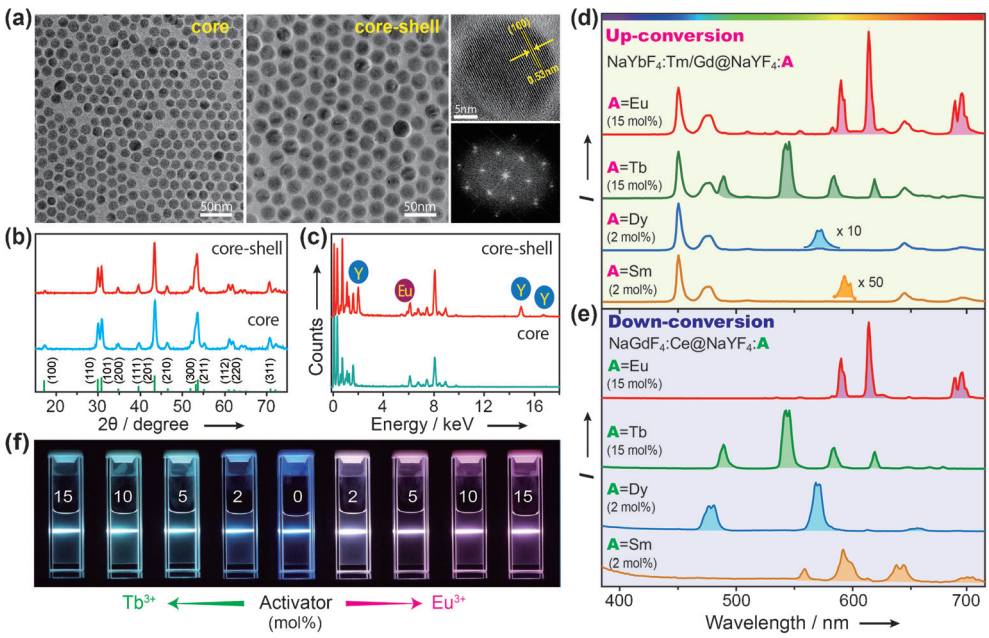

Figure 2. a) TEM images, b) X-ray diffraction (XRD) patterns, and c) energy-dispersive X-ray spectroscopy (EDS) of as-synthesized $NaYbF_4$:Tm/Gd(1/50 mol%) core and $NaYbF_4$:Tm/Gd(1/50 mol%)@$NaYF_4$:Eu-(15 mol%) core–shell nanoparticles. Right panels of (a) show the high-resolution TEM image (top) and corresponding Fourier transform diffraction pattern (bottom) of the core–shell sample. Note that the diffraction pattern data plotted at the bottom of (b) is from a hexagonal phase $NaYF_4$ crystal (JCPDS #16-0334). d) Up-conversion emission spectra of $NaYbF_4$:Tm/Gd(1/50 mol%)@$NaYF_4$:A (A = Eu, Tb, Dy, and Sm) core–shell nanocrystals under 980 nm excitation. e) Down-conversion emission spectra of $NaGdF_4$:Ce-(15 mol%)@$NaYF_4$:A(A = Eu, Tb, Dy, and Sm) core–shell nanocrystals under 254 nm excitation. f) Emission color tuning of $NaYbF_4$:Tm/Gd(1/50 mol%)@$NaYF_4$:A(A = Eu or Tb) core–shell nanoparticles by varying the concentration of emitters doped in the shell layer.

$NaYbF_4$:Tm/Gd/A@$NaYF_4$ and $NaCeF_4$:Gd/A@$NaYF_4$. Notably, their emission is too weak to be recorded (for upconversion) or much weaker (for down-conversion) than that obtained through the interfacial energy transfer (Figure S10). By tuning the species and content of lanthanide dopants doped in the shell layer, multiple emission colors were obtained (Figure 2 f). These experimental investigations have definitely confirmed the core–shell interfacial energy transfer as an efficient approach to achieve photon up- and down-conversion of lanthanide-doped nanocrystals.

We next investigated the spatial scope of the Gd^{3+}-mediated interfacial energy transfer leading to the photon emission. Because the interactions between lanthanide ions are sensitively dependent on their separation,[7] the interfacial energy transfer would be closely constrained in a narrow layer away from the core/shell interface (Scheme A in Figure 3 a). For a quantitative study, we design a core–shell–shell structure with a thickness-tunable interlayer between the core and optically inactive outer shell layer, for example, $NaYbF_4$:Tm/Gd@$NaYF_4$:A@$NaYF_4$ (A = Eu and Tb) for up-conversion and $NaGdF_4$:Ce@$NaYF_4$:A@$NaYF_4$ (A = Eu and Tb) for down-conversion (Scheme B in Figure 3 a). Their emission spectra (Figure 3 b,c) show a rapid rise in intensity as the interlayer thickness increases from 0 to approximately 1.5 nm, and then approaches to the emission intensity comparable to that of the commonly synthesized core–shell samples with further increasing the interlayer thickness. These results have revealed that the Gd^{3+}-mediated interfacial energy transfer is primarily confined in an approximately 1.5 nm thick layer away from the core/shell interface.

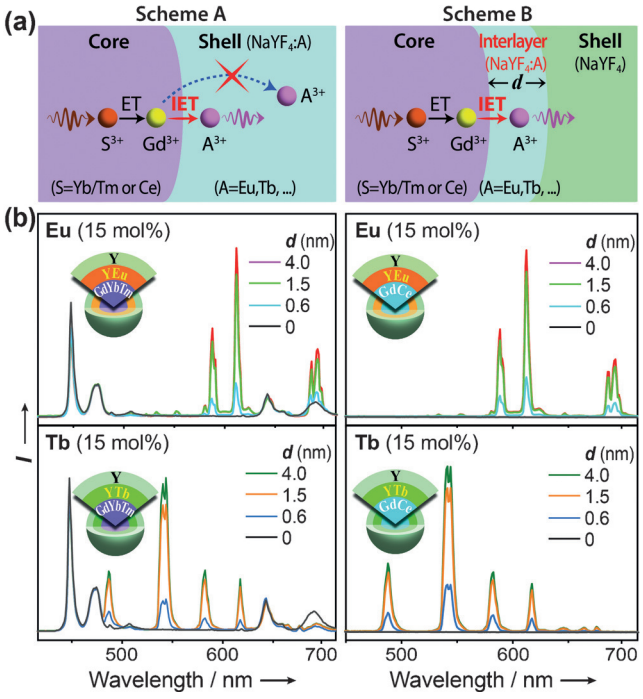

Figure 3. a) Mechanistic study of Gd^{3+}-mediated interfacial energy transfer. Scheme A: Incapability of interfacial energy transfer for activating the lanthanide emitters in the shell layer further away from the core/shell interface; Scheme B: Proposed core–shell–shell structure with a thickness-variable inter-layer for investigating the spatial scope of interfacial energy transfer. b) Up-conversion emission spectra (left panel) obtained from $NaYbF_4$:Tm/Gd(1/50 mol%)@$NaYF_4$:A(A = Eu,Tb; 15 mol%)@$NaYF_4$ and down-conversion emission spectra (right panel) obtained from $NaGdF_4$:Ce(15 mol%)@$NaYF_4$:A(A = Eu,Tb; 15 mol%)@$NaYF_4$ core–shell–shell nanoparticles with different thickness of $NaYF_4$:A interlayer (*d*:0–4.0 nm). Note that emission spectra data from $NaYbF_4$:Tm/Gd(1/50 mol%)@$NaYF_4$ and $NaGdF_4$:Ce(15 mol%)@$NaYF_4$ core–shell samples were used when *d* is 0 nm.

Since the recent observation of a similar emission phenomenon in energy-migratory $NaGdF_4$@$NaGdF_4$ core–shell system,[1e] undertaking a comparative study of it with the present work has become of great importance. In this case, we synthesized a series of control samples of $NaGdF_4$:Yb/Tm(49/1 mol%)@$NaXF_4$:A (X = Y, Gd; A = Eu, Tb; 15 mol%) and measured their emission spectra. Note that the nanoparticles $NaGdF_4$:Yb/Tm(49/1 mol%)@$NaXF_4$:A and $NaYbF_4$:Tm/Gd(1/50 mol%)@$NaXF_4$:A are the same samples with different names. As shown in Figure 4 a, the up-conversion emissions were indeed obtained in these core–shell samples under 980 nm excitation, and more importantly, the emission intensity is slightly enhanced for the samples coated with $NaYF_4$:A shell layer, being consistent with the longer decay times obtained from the same samples (Figure S11). We further synthesized the $NaGdF_4$:Ce(15 mol%)@$NaXF_4$:A (X = Y, Gd; A = Eu, Tb; 15 mol%) core–shell nanoparticles and their down-conversion spectra show a similar change tendency as those obtained from the up-conversion samples (Figures S12,S13). These results indicate that the emission of lanthanide emitters embedded in shell layer may not essentially depend on the migration in the $NaGdF_4$ shell matrix. Therefore, further study is required regarding the contribution of Gd^{3+}→Gd^{3+} energy migration to the photon emission of lanthanide emitters for the $NaGdF_4$@$NaGdF_4$ type samples.

Aiming to distinguish the energy migration and energy transfer both of which take place for the $NaGdF_4$@$NaGdF_4$ type samples, we propose a core–shell–shell structure design by coating a $NaYF_4$:Tb shell layer outside these core–shell samples (see Figure 4 b). It is found that the energy transfer from Eu^{3+} to Tb^{3+} seldom occurs while it from Gd^{3+} to Tb^{3+} is easily available (Figure S14), allowing us to detect the energy migration occurring within the interlayer by measurement of the Tb^{3+} emission. Control tri-layer samples including $NaGdF_4$:Yb/Tm@$NaGdF_4$:Eu@$NaYF_4$:Tb and $NaGdF_4$:Ce@$NaGdF_4$:Eu@$NaYF_4$:Tb were synthesized, and their emission spectra are shown in Figure 4 c. Intriguingly, the emission of Tb^{3+} is very strong for the tri-layer samples with the $NaGdF_4$ interlayer as a result of energy migration, however, it nearly vanishes for the samples doped with Eu^{3+} in the interlayer, in particular with up-conversion. This suggests an existence of competitions between the interfacial energy transfer and energy migration (Stages I and II in Figure 4 b), subsequently making the energy difficult to migrate over an approximately 4.0 nm thick $NaGdF_4$ interlayer at the presence of Eu^{3+} in this layer. In an attempt to further probe the energy migration, we prepared the tri-layer samples with a smaller $NaGdF_4$:Eu interlayer thickness. Their spectral result shows a rapid decrease of Tb^{3+} emission intensity with the increase in the interlayer thickness (Fig-

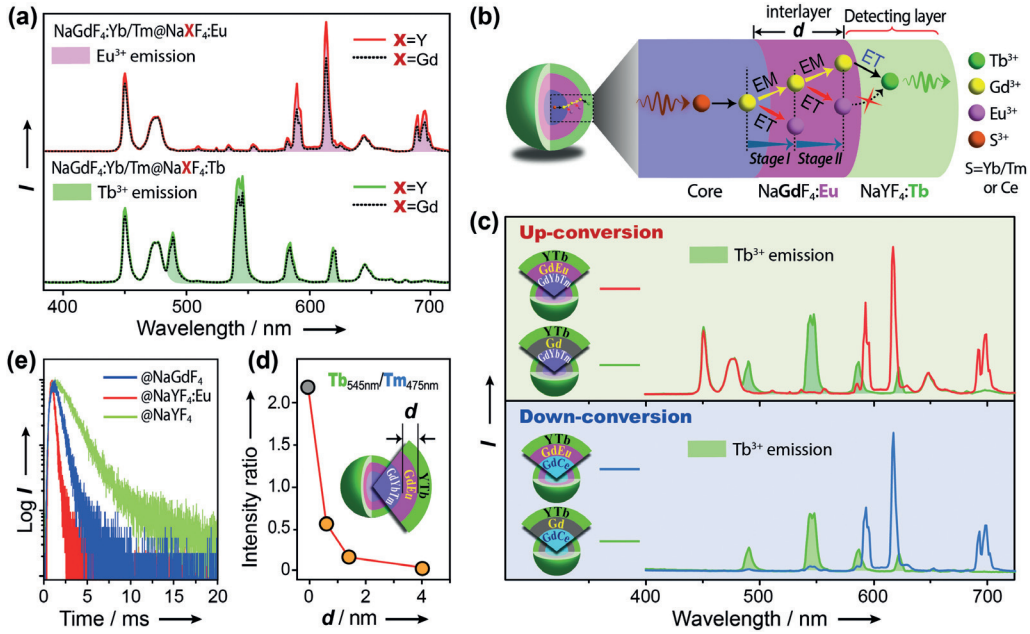

Figure 4. a) Up-conversion emission spectra of $NaGdF_4$:Yb/Tm(49/1 mol%)@$NaXF_4$:A (X = Y,Gd; A = Eu,Tb; 15 mol%) core–shell nanocrystals under 980 nm excitation. b) Schematic of proposed core–shell–shell structure design for investigation of $Gd^{3+}\rightarrow Gd^{3+}$ energy migration by detecting the Tb^{3+} emission from the outermost shell layer. EM = energy migration, ET = energy transfer. c) Up-conversion emission spectra of $NaGdF_4$:Yb/Tm(49/1 mol%)@$NaGdF_4$:Eu(15 mol%)@$NaYF_4$:Tb(15 mol%) and down-conversion emission spectra of $NaGdF_4$:Ce-(15 mol%)@$NaGdF_4$:Eu(15 mol%)@$NaYF_4$:Tb(15 mol%) core–shell–shell nanoparticles. Note that the emission spectra of the core–shell–shell samples without Eu^{3+} in the interlayer are also plotted for comparison. d) Luminescence intensity of Tb^{3+} emission at 545 nm ($^5D_0\rightarrow{}^7F_2$ transition) as a function of the $NaGdF_4$:Eu interlayer thickness (*d*) for the $NaGdF_4$:Yb/Tm@$NaGdF_4$:Eu@$NaYF_4$:Tb samples under 980 nm excitation. Note that the emission intensity of Tb^{3+} is normalized to the blue emission of Tm^{3+} at 475 nm ($^1G_4\rightarrow{}^3H_6$ transition). e) Decay curves of Gd^{3+} emission at 311 nm ($^6P_{7/2}\rightarrow{}^8S_{7/2}$ transition) from the $NaGdF_4$:Yb/Tm@$NaYF_4$, $NaGdF_4$:Yb/Tm@$NaYF_4$:Eu and $NaGdF_4$:Yb/Tm@$NaGdF_4$ core–shell samples under a pulsed 980 nm laser excitation.

ure 4d), implying that the energy migration only works within a narrow layer close to the core/shell interface. More importantly, the very weak Tb^{3+} emission recorded from these samples confirmed that the photon emission of emitters within the $NaGdF_4$ shell layer is mainly produced by the interfacial energy transfer rather than energy migration.

To shed more light on the mechanistic origin that leads to the difference between the two energy interactions, we measured the decay curve of Gd^{3+} emission at wavelength of 311 nm ($^6P_{7/2}\rightarrow{}^8S_{7/2}$ transition). The lifetime of Gd^{3+} at its $^6P_{7/2}$ state for the sample coated with a $NaGdF_4$ layer is clearly shorter than that coated with an outer $NaYF_4$ layer due to energy migration (Figure 4e). However, it is still much longer compared to that of the samples with emitters doped in the shell layer (i.e., $NaGdF_4$:Yb/Tm@$NaYF_4$:Eu), intrinsically confirming much less efficient energy migration than energy transfer at the core/shell interfacial area. This difference in nature may be ascribed to the physical requirement for an efficient energy transfer in which a much shorter decay time of donor than that of the acceptor is a necessary condition.[2a,7] In the present work, the lifetime of Gd^{3+} is 2.38 ms, much shorter than the emitters (e.g., 5.58 ms for Eu^{3+}), allowing an easier transfer from the energy stored Gd^{3+} to a nearby lanthanide emitter instead of to a Gd^{3+} as in the $NaGdF_4$:A layered samples. Taken together, these results have clearly evidenced the priority of interfacial energy transfer over the energy migration in achieving photon emission for the $NaGdF_4$@$NaGdF_4$ type systems.

In conclusion, we have mechanistically demonstrated a novel and efficient energy-manipulating strategy for achieving photon up- and down-conversion through Gd^{3+}-mediated interfacial energy transfer. We have also examined and confirmed the dominance of interfacial energy transfer over the energy migration in gaining photon emission for the $NaGdF_4$@$NaGdF_4$ type system. These discoveries provide a deeper mechanistic understanding of the fundamental processes involving lanthanide interactions on the nanometer-length scale. More importantly, they are able to pave a new way to control and modify the photon emission of lanthanide-doped materials and consequently contribute to their frontier applications.

Acknowledgements

This work was supported by The Hong Kong Polytechnic University Funds (1-ZE14, 1-ZVGH) and the National Natural Science Foundation of China (Grant No. 51472088).

Keywords: core–shell architecture · down-conversion · interfacial energy transfer · lanthanides · up-conversion

How to cite: *Angew. Chem. Int. Ed.* **2016**, *55*, 12356–12360
Angew. Chem. **2016**, *128*, 12544–12548

[1] a) B. Zhou, B. Shi, D. Jin, X. Liu, *Nat. Nanotechnol.* **2015**, *10*, 924; b) R. T. Wegh, H. Donker, K. D. Oskam, A. Meijerink, *Science* **1999**, *283*, 663; c) D. J. Gargas, E. M. Chan, A. D. Ostrowski, S. Aloni, M. V. P. Altoe, E. S. Barnard, B. Sanii, J. J. Urban, D. J. Milliron, B. E. Cohen, P. J. Schuck, *Nat. Nanotechnol.* **2014**, *9*, 300; d) E. M. Chan, G. Han, J. D. Goldberg, D. J. Gargas, A. D. Ostrowski, P. J. Schuck, B. E. Cohen, D. J. Milliron, *Nano Lett.* **2012**, *12*, 3839; e) F. Wang, R. Deng, J. Wang, H. Wang, Y. Han, H. Zhu, X. Chen, X. Liu, *Nat. Mater.* **2011**, *10*, 968; f) C. Yan, A. Dadvand, F. Rosei, D. F. Perepichka, *J. Am. Chem. Soc.* **2010**, *132*, 8868; g) H. H. Gorris, O. S. Wolfbeis, *Angew. Chem. Int. Ed.* **2013**, *52*, 3584; *Angew. Chem.* **2013**, *125*, 3668; h) C. Zhang, H.-P. Zhou, L.-Y. Liao, W. Feng, W. Sun, Z.-Y. Li, C.-H. Xu, C.-J. Fang, L.-D. Sun, Y.-W. Zhang, C.-H. Yan, *Adv. Mater.* **2010**, *22*, 633; i) Y. Lu, J. Zhao, R. Zhang, Y. Liu, D. Liu, E. Goldys, X. Yang, P. Xi, A. Sunna, J. Lu, Y. Shi, R. C. Leif, Y. Huo, J. Shen, J. A. Piper, J. P. Robinson, D. Jin, *Nat. Photonics* **2013**, *8*, 32; j) Y. Tang, W. Di, X. Zhai, R. Yang, W. Qin, *ACS Catal.* **2013**, *3*, 405; k) B. S. Richards, *Sol. Energy Mater. Sol. Cells* **2006**, *90*, 2329; l) J. M. Meruga, A. Baride, W. Cross, J. J. Kellar, P. S. May, *J. Mater. Chem. C* **2014**, *2*, 2221; m) T. He, W. Wei, L. Ma, R. Chen, S. Wu, H. Zhang, Y. Yang, J. Ma, L. Huang, G. G. Gurzadyan, H. Sun, *Small* **2012**, *8*, 2163; n) R. Deng, F. Qin, R. Chen, W. Huang, M. Hong, X. Liu, *Nat. Nanotechnol.* **2015**, *10*, 237; o) N. M. Idris, M. K. Gnanasammandhan, J. Zhang, P. C. Ho, R. Mahendran, Y. Zhang, *Nat. Med.* **2012**, *18*, 1580; p) L. Zhou, R. Wang, X. Li, C. Yao, C. Wang, X. Zhang, C. Xu, A. Zeng, D. Zhao, F. Zhang, *Nat. Commun.* **2015**, *6*, 6938; q) P. Rodríguez-Sevilla, Y. Zhang, P. Haro-González, F. Sanz-Rodríguez, F. Jaque, J. G. Solé, X. Liu, D. Jaque, *Adv. Mater.* **2016**, *28*, 2421.

[2] a) F. Auzel, *Chem. Rev.* **2004**, *104*, 139; b) M. Haase, H. Schäfer, *Angew. Chem. Int. Ed.* **2011**, *50*, 5808; *Angew. Chem.* **2011**, *123*, 5928; c) G. Liu, *Chem. Soc. Rev.* **2015**, *44*, 1635.

[3] C. Renero-Lecuna, R. Martín-Rodríguez, R. Valiente, J. González, F. Rodríguez, K. W. Krämer, H. U. Güdel, *Chem. Mater.* **2011**, *23*, 3442.

[4] a) S. Heer, K. Kompe, H. U. Gudel, M. Haase, *Adv. Mater.* **2004**, *16*, 2102; b) S. Sivakumar, F. C. J. M. van Veggel, M. Raudsepp, *J. Am. Chem. Soc.* **2005**, *127*, 12464; c) B. Zhou, L. Tao, Y. H. Tsang, W. Jin, *J. Mater. Chem. C* **2013**, *1*, 4313; d) Y. Liu, D. Tu, H. Zhu, R. Li, W. Luo, X. Chen, *Adv. Mater.* **2010**, *22*, 3266; e) G. Wang, Q. Peng, Y. Li, *J. Am. Chem. Soc.* **2009**, *131*, 14200; f) X. Xie, N. Gao, R. Deng, Q. Sun, Q.-H. Xu, X. Liu, *J. Am. Chem. Soc.* **2013**, *135*, 12608; g) V. Mahalingam, F. Mangiarini, F. Vetrone, V. Venkatramu, M. Bettinelli, A. Speghini, J. A. Capobianco, *J. Phys. Chem. C* **2008**, *112*, 17745; h) G. Chen, J. A. Damasco, H. Qiu, W. Shao, T. Y. Ohulchanskyy, R. R. Valiev, X. Wu, G. Han, Y. Wang, C. Yang, H. Ågren, P. N. Prasad, *Nano Lett.* **2015**, *15*, 7400; i) T. Yang, Y. Sun, Q. Liu, W. Feng, P. Yang, F. Li, *Biomaterials* **2012**, *33*, 3733; j) J. Wang, T. Ming, Z. Jin, J. Wang, L. D. Sun, C. H. Yan, *Nat. Commun.* **2014**, *5*, 5669; k) J. Wang, R. Deng, M. A. MacDonald, B. Chen, J. Yuan, F. Wang, D. Chi, T. S. A. Hor, P. Zhang, X. Liu, *Nat. Mater.* **2014**, *13*, 157; l) J. Zhou, G. Chen, E. Wu, G. Bi, B. Wu, Y. Teng, S. Zhou, J. Qiu, *Nano Lett.* **2013**, *13*, 2241; m) Y. Zhong, G. Tian, Z. Gu, Y. Yang, L. Gu, Y. Zhao, Y. Ma, J. Yao, *Adv. Mater.* **2014**, *26*, 2831; n) B. Zhou, W. Yang, S. Han, Q. Sun, X. Liu, *Adv. Mater.* **2015**, *27*, 6208; o) T. Y. Ohulchanskyy, R. R. Valiev, X. Wu, G. Han, Y. Wang, C. Yang, H. Ågren, P. N. Prasad, *Nano Lett.* **2015**, *15*, 7400; p) X. Li, Z. Guo, T. Zhao, Y. Lu, L. Zhou, D. Zhao, F. Zhang, *Angew. Chem. Int. Ed.* **2016**, *55*, 2464; *Angew. Chem.* **2016**, *128*, 2510.

[5] a) H. Meyssamy, K. Riwotzki, A. Kornowski, S. Naused, M. Haase, *Adv. Mater.* **1999**, *11*, 840; b) P. Li, Q. Peng, Y. Li, *Adv. Mater.* **2009**, *21*, 1945; c) J. R. DiMaio, B. Kokuoz, J. Ballato, *Opt. Express* **2006**, *14*, 11412; d) Z. L. Wang, Z. W. Quan, P. Y. Jia, C. K. Lin, Y. Luo, Y. Chen, J. Fang, W. Zhou, C. J. O'Connor, J. Lin, *Chem. Mater.* **2006**, *18*, 2030; e) S. Y. Kim, K. Woo, K. Lim, K. Lee, H. S. Jang, *Nanoscale* **2013**, *5*, 9255; f) D. Peng, Q. Ju, X. Chen, R. Ma, B. Chen, G. Bai, J. Hao, X. Qiao, X. Fan, F. Wang, *Chem. Mater.* **2015**, *27*, 3115.

[6] a) L. Wang, Y. Li, *Chem. Mater.* **2007**, *19*, 727; b) R. Kumar, M. Nyk, T. Y. Ohulchanskyy, C. A. Flask, P. N. Prasad, *Adv. Funct. Mater.* **2009**, *19*, 853.

[7] a) D. L. Dexter, *J. Chem. Phys.* **1953**, *21*, 836; b) L. G. van Uitert, L. F. Johnson, *J. Chem. Phys.* **1966**, *44*, 3514; c) L. V. G. Tarelho, L. Gomes, I. M. Ranieri, *Phys. Rev. B* **1997**, *56*, 14344; d) F. Vetrone, J.-C. Boyer, J. A. Capobianco, A. Speghini, M. Bettinelli, *J. Appl. Phys.* **2004**, *96*, 661.

Received: May 13, 2016
Published online: July 5, 2016

